ON THE ORIENTATION OF CRYSTALS IN PORPHYRITIC ROCKS

By

F. Richard Yeatts

Department of Physics, University of Arizona

INTRODUCTION

In certain igneous rocks, such as porphyries, relatively large inclusions are found imbedded in a fine-grained groundmass; and, such inclusions are often observed to be at least partially aligned. Furthermore, this aligning can sometimes be attributed solely to a process of deformation that the rock underwent while still somewhat mobile. The case where the deformation is thought to have occurred before the groundmass was completely solidified, but after the phenocrysts were well formed, has been considered by such workers as Riedel (1929), March (1932), and Oertel (1955). The research discussed in this paper forms an extension of their work.

The paper is divided into three parts: In the first, a mathematical theory is developed for predicting the type of alignment produced by uniform deformation. In the second part, examples of the mathematical theory are presented for the cases of flake-shaped, splinter-shaped, and ellipsoidal inclusions. The third part deals with the application of the general theory to a particular geological formation—the Large Phenocrysts Porphyry described by Mayo (1961).

MATHEMATICAL THEORY

In this section, as well as under the heading "Examples," the mathematical background for describing the orientations of solid inclusions in deforming plastic media is developed in some detail. This should be of interest to those concerned with the mechanics of such deformations. Readers not interested in the theory but wishing to know the results of its application was advised to skip the next two sections and begin reading under the heading "Applications."

When a rock, such as the Large Phenocryst Porphyry, is observed in the field, only its surface is available for study; the spatial orientations of its inclusions must be inferred from the planar orientations of their exposed sections. When the aligning is not so prominent that directional tendencies are obvious, the standard method for depicting such tendencies is through the use of rose diagrams. The rose diagram is simply a polar plot of the number of inclusions versus direction of their planar orientation; usually, the orientations measured for all inclusions in a given circular region are included in the plot. If the orientations of the inclusions were completely random, the representative rose diagram would be circular.

The problem at hand is to determine theoretically the shape of a rose diagram in the case where the observed alignment was produced solely by a plastic deformation of the mobile groundmass. It is assumed that the inclusions are rigid and were randomly oriented before deformation. It is further required that all inclusions be similarly shaped, although not necessarily the same size. Also, there must be sufficient spacing between inclusions so that the relative rotation of any one inclusion interferes but negligibly with the rotation of any other. Finally, it is stipulated that the deformation be "uniform" over the entire region of interest; that is, any two inclusions that were oriented relatively the same before deformation must be oriented relatively the same afterwards, regardless of their locations in the region.

Formally it is necessary to consider just one inclusion, oriented at random initially, and imbedded in an infinite plastic medium. By prescribing the strain of the medium at infinity, and the nature of its plasticity, one can, in principle, determine the final orientation of the inclusion if its initial orientation is known. And further, one can then determine the probability of finding the inclusion in any particular final orientation on the basis of its initial random orientation. Let it be emphasized here that it is not the spatial orientation of the inclusion that is of ultimate interest but the planar orientation of a cross section of the inclusion. In practice the sectioning plane would be the surface of the rock.

Let the orientation of the inclusion be specified by the angles: Θ, Φ, Ψ, measured with respect to a Cartesian coordinate system whose xy-plane is the sectioning plane, and whose origin is on the "principal axis" of the inclusion. The "principal axis" is simply a characteristic line through the inclusion, such as a largest dimension or a symmetry axis. In figure 1 an ellipsoidal inclusion is illustrated: The longest axis is defined as the principal axis; "Θ" measures the angle between the principal axis and the z-axis; "Φ" measures the angle between the projection of the principal axis on the xy-plane and the x-axis; and "Ψ" measures the angle by which a second characteristic axis, for example the shortest axis of the ellipsoid, is rotated about the principal axis from the xy-plane.

For the initial condition of randomness, one can write:

$$d^3P = \frac{1}{8\pi^2} \sin\Theta \, d\Theta \, d\Phi \, d\Psi \qquad (1)$$

The probability "d^3P" of finding the principal axis of the inclusion between "Θ, $\Theta + d\Theta$" and "Φ, $\Phi + d\Phi$" and its second characteristic axis between "Ψ, $\Psi + d\Psi$" depends only on the size of the solid angle "$\sin\Theta \, d\Theta \, d\Phi$" and the size of the increment of rotation "$d\Psi$." The factor "$\frac{1}{8\pi^2}$" is the normalization constant.

Consider now some strain in the medium surrounding the inclusion, causing it to be rotated to the new position: "Θ', Φ', Ψ'." Let the inclusion be sectioned now by the xy-plane; define "$\bar{\Phi}$" to be the planar orientation of the cross section measured from the x-axis to a characteristic line in the cross section. For the ellipsoid pictured in figure 1, the characteristic line would be the major axis of the ellipse cut out by the xy-plane. The angle "$\bar{\Phi}$" can be written as a function of the final angles "Θ', Φ', Ψ'," but these in turn can be written as functions of the initial angles "Θ, Φ, Ψ" and the parameters descriptive of the strain; thus:

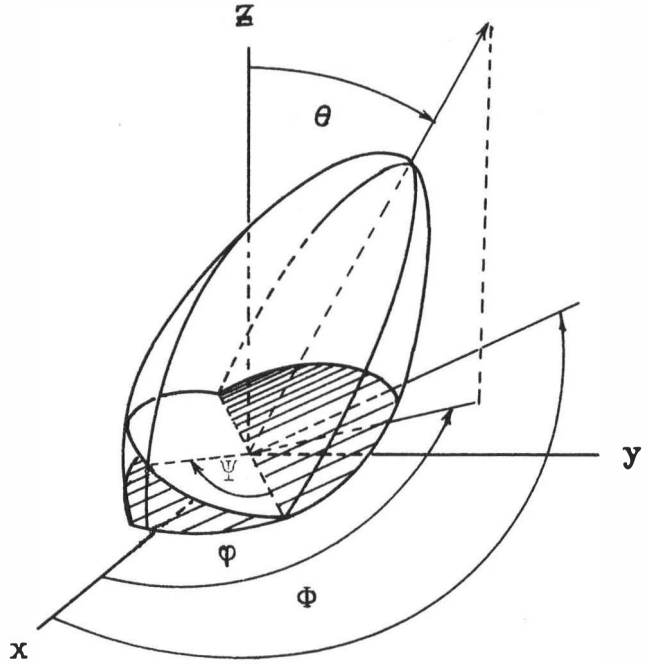

Figure 1. --Location of axes on ellipsoidal inclusion.

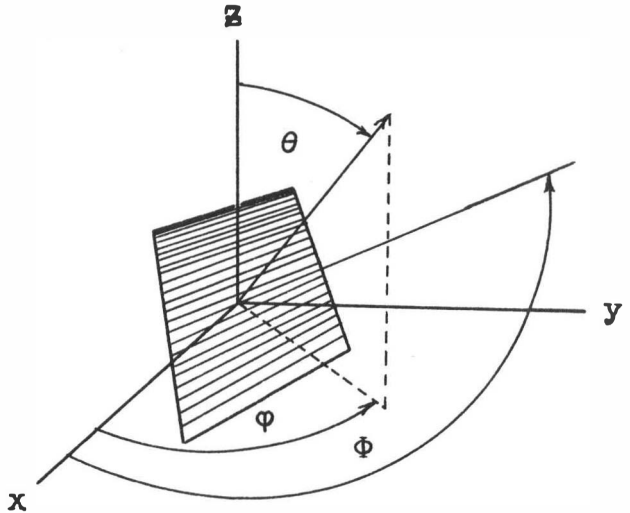

Figure 2. --Angular relationships for a plane.

$$\Phi = \Phi(\theta, \phi, \psi \text{ ; strain parameters}) \tag{2}$$

The above relation can be looked upon as a change in variables. Then, if it is possible to invert the expression and solve explicitly for one of the initial angles, say "ϕ," the probability "d^3P" can be written:

$$d^3P = \frac{1}{8\pi^2} \sin\theta \left(\frac{\delta\phi}{\delta\Phi}\right) d\theta\, d\Phi\, d\psi \tag{3}$$

$$\phi = \phi(\theta, \Phi, \psi \text{ ; strain parameters})$$

If now an integration is performed over the two initial angles, one has:

$$dP = \rho(\Phi)\, d\Phi \tag{4}$$

$$\rho(\Phi) = \int_0^{\pi} \sin\theta \int_0^{2\pi} \left(\frac{\delta\phi}{\delta\Phi}\right) d\psi\, d\theta \tag{5}$$

The function "$\rho(\Phi)$" depends on "Φ," of course, and the strain parameters. "dP" is the probability of finding the inclusion with its final planar orientation between "Φ, $\Phi + d\Phi$"; when plotted on polar paper "$\rho(\Phi)$" is just the desired rose diagram.

EXAMPLES

When a homogeneous plastic medium is strained uniformly, the deformation is described by the affine transformation:

$$\begin{aligned} x' &= (1 + e_{11})x + e_{12}y + e_{13}z \\ y' &= e_{21}x + (1 + e_{22})y + e_{23}z \\ z' &= e_{31}x + e_{32}y + (1 + e_{33})z \end{aligned} \tag{6}$$

"x', y', z'" give the position of a point in the medium whose coordinates before deformation were "x, y, z." The numbers "$e_{11}, e_{12}, \ldots, e_{33}$" are called the components of the strain and are constants when the deformation is uniform. It is easily shown that under an affine transformation, straight lines are transformed into straight lines and planes are transformed into planes.

Consider the presence of rigid flake-shaped (or splinter-shaped) inclusions in the medium. It would seem reasonable to expect that if the same stress which originally produced the uniform deformation were now applied to the medium, that the deformation would still be uniform except in the immediate vicinity of an inclusion, and that the inclusion would be rotated in much the same way as was the plastic medium it displaced. These expectations have been verified experimentally by the author in the two dimensional case. Segments of fine wire were imbedded in the surface of a clay cake at preassigned

orientations. Upon deforming the cake uniformly, it was found that the wires were rotated the same amount as a set of similarly oriented straight lines merely ruled on the surface. It will thus be assumed that in three dimensions also, rigid flake-shaped (or splinter-shaped) particles will rotate under uniform deformation precisely as the mathematical planes (or lines) they lie along.

Turning first to the case of flake-shaped particles, let the spherical angles "Θ, Φ" locate the normal to the plane which one such particle lies along before deformation. The equation of this plane is given by:

$$x \sin\Theta\cos\Phi + y \sin\Theta\sin\Phi + Z \cos\Theta = 0 \tag{7}$$

From figure 2 it is apparent that "Θ" is just the dip of the plane with respect to the xy-plane, and "$\Phi + \frac{\pi}{2}$" is its strike. After deformation the plane has the formula:

$$x' \sin\Theta' \cos\Phi' + y' \sin\Theta' \sin\Phi' + Z' \cos\Theta' = 0 \tag{8}$$

When sectioned along the xy-plane, a flake-shaped particle will leave as its trace a "line segment" in the direction of strike; call this direction "$\bar{\Phi}$":

$$\bar{\Phi} = \Phi' + \frac{\pi}{2} \tag{9}$$

To express "Φ'" in terms of "Θ, Φ" and the strain parameters, introduce the inverse transformation of "6":

$$\begin{aligned} x &= (1 + a_{11})x' + a_{12}\, y' + a_{13}\, Z' \\ y &= a_{21}\, x' + (1 + a_{22})y' + a_{23}\, Z' \\ Z &= a_{31}\, x' + a_{32}\, y' + (1 + a_{33})Z' \end{aligned} \tag{10}$$

The inverse transformation exists as long as the determinant of the coefficients of equation "6" does not vanish:

$$\det \begin{vmatrix} (1 + e_{11}) & e_{12} & e_{13} \\ e_{21} & (1 + e_{22}) & e_{23} \\ e_{31} & e_{32} & (1 + e_{33}) \end{vmatrix} \neq 0 \tag{11}$$

This determinant, however, is a measure of volume dialation, and its vanishing would imply that volume has been annihilated by the deformation... a physical impossibility. For incompressible materials the determinant equals unity.

Substituting from "10" into "7" and rearranging gives:

$$\left[(1 + a_{11})\sin\theta\cos\phi + a_{21}\sin\theta\sin\phi + a_{31}\cos\theta\right]x' + \left[a_{12}\sin\theta\cos\phi + (1 + a_{22})\sin\theta\sin\phi + a_{32}\cos\theta\right]y' + \left[a_{13}\sin\theta\cos\phi + a_{23}\sin\theta\sin\phi + (1 + a_{33})\cos\theta\right]Z' = 0 \quad (12)$$

Comparing equation "12" with "8" it is possible to write:

$$\tan\phi' = \frac{a_{12}\sin\theta\cos\phi + (1 + a_{22})\sin\theta\sin\phi + a_{32}\cos\theta}{(1 + a_{11})\sin\theta\cos\phi + a_{21}\sin\theta\sin\phi + a_{31}\cos\theta} \quad (13)$$

And the orientation of the section " Φ " is given by:

$$\Phi = \tan^{-1}\left[\frac{a_{12}\sin\theta\cos\phi + (1 + a_{22})\sin\theta\sin\phi + a_{32}\cos\theta}{(1 + a_{11})\sin\theta\cos\phi + a_{21}\sin\theta\sin\phi + a_{31}\cos\theta}\right] + \frac{\pi}{2} \quad (14)$$

According to the general theory, one must now solve equation "14" for one of the original angles, in this case "ϕ," and form "$\frac{\delta\theta}{\delta\Phi}$":

$$\theta = -\tan^{-1}\left[\frac{a_{32}\sin\Phi + a_{31}\cos\Phi}{(a_{12}\cos\phi + (1 + a_{22})\sin\phi)\sin\Phi + ((1+a_{11})\cos\phi + a_{21}\sin\phi)\cos\Phi}\right] \quad (15)$$

$$\frac{\delta\theta}{\delta\Phi} = \frac{((1+a_{22})a_{31} - a_{21}a_{32})\sin\phi + (a_{12}a_{31} - (1+a_{11})a_{32})\cos\phi}{\left[((1+a_{22})\sin\Phi + a_{21}\cos\Phi)\sin\phi + (a_{12}\sin\Phi + (1+a_{11})\cos\Phi)\right]^2 + \left[a_{32}\sin\Phi + a_{31}\cos\Phi\right]^2} \quad (16)$$

And also, it is necessary to have:

$$\sin\theta = \frac{a_{32}\sin\Phi + a_{31}\cos\Phi}{\left\{\left[((1+a_{22})\sin\Phi + a_{21}\cos\Phi)\sin\phi + (a_{12}\sin\Phi + (1+a_{11})\cos\Phi)\right]^2 + \left[a_{32}\sin\Phi + a_{31}\cos\Phi\right]^2\right\}^{1/2}} \quad (17)$$

Then we form the integral:

$$\rho(\Phi) = \frac{1}{8\pi^2}\int_0^{2\pi}\sin\theta\left(\frac{\delta\theta}{\delta\Phi}\right)d\phi\int_0^{2\pi}d\psi \quad (18)$$

which evaluates to:

$$\rho(\Phi) = \frac{1}{4\pi} \frac{1}{A\sin^2\Phi + 2B\sin\Phi\cos\Phi + C\cos^2\Phi} \times \left\{ \frac{\mathcal{M}_1 \sin\Phi + \lambda_1 \cos\Phi}{\sqrt{\alpha_1\sin^2\Phi + 2\beta_1\sin\Phi\cos\Phi + r_1\cos^2\Phi}} + \frac{\mathcal{M}_2 \sin\Phi + \lambda_2 \cos\Phi}{\sqrt{\alpha_2\sin^2\Phi + 2\beta_2\sin\Phi\cos\Phi + r_2\cos^2\Phi}} \right\} \tag{19}$$

where:

$$A = a_{12}^2 + (1+a_{22})^2 + a_{32}^2 \qquad B = (1+a_{11})a_{12} + a_{21}(1+a_{22}) + a_{31}a_{32} \qquad C = (1+a_{11})^2 + a_{21}^2 + a_{31}^2$$

$$\alpha_1 = a_{12}^2 + a_{32}^2 \qquad \beta_1 = (1+a_{11})a_{12} + a_{31}a_{32} \qquad r_1 = (1+a_{11})^2 + a_{31}^2$$

$$\alpha_2 = (1+a_{22})^2 + a_{32}^2 \qquad \beta_2 = (1+a_{22})a_{21} + a_{32}a_{31} \qquad r_2 = a_{21}^2 + a_{31}^2$$

$$\mathcal{M}_1 = E_1a_{32} - E_3a_{12} \qquad \lambda_1 = E_1a_{31} - E_3(1+a_{11})$$

$$\mathcal{M}_2 = E_2a_{32} + E_3(1+a_{22}) \qquad \lambda_2 = E_2a_{31} + E_3a_{21}$$

$$E_1 = -\det \begin{vmatrix} a_{21} & (1+a_{22}) \\ a_{31} & a_{32} \end{vmatrix} \qquad E_2 = -\det \begin{vmatrix} (1+a_{11}) & a_{12} \\ a_{31} & a_{32} \end{vmatrix} \qquad E_3 = -\det \begin{vmatrix} (1+a_{11}) & a_{12} \\ a_{21} & (1+a_{22}) \end{vmatrix}$$

Equation "19" is the desired formula for predicting the rose diagram appropriate to flake-shaped particles. To interpret this result, however, it is well to consider particular examples. In figures 3, 4, and 5, polar plots of "$\rho(\Phi)$" are presented for three simple but representative types of strain: simple extension in the x-direction, shear in the xy-plane, and shear in the xz-plane. The effects of different magnitudes of strain are illustrated in the case of simple extension.

A few remarks can be made about the functional behavior of equation "19." First of all, the symmetry requirement:

$$\rho(\Phi + \pi) = \rho(\Phi) \tag{20}$$

can be met by merely choosing the appropriate signs for the square roots. Secondly, the possibility that one of the denominators might vanish is not a serious difficulty. For the first denominator on the right to equal zero, the three coefficients "E_1, E_2, E_3" must all equal zero; but this implies that volume was annihilated by the deformation. The vanishing of the other two denominators can occur only if "E_1" in the one case or "E_2" in the other were to vanish; and in addition, the vanishing only occurs at a particular angle. But at this angle the numerators will, in each case, also vanish; the resulting indeterminancy is but a removable singularity.

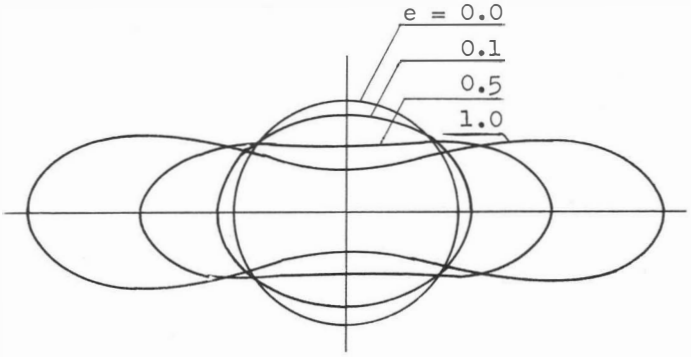

$1+e_{11}=1+e,\ 1+e_{22}=1+e_{33}=\frac{1}{1+e},\quad e_{ij}=0 \text{ for } i\neq j$

$$\rho(\Phi)\triangleq \frac{(1+e)^{3/2}}{2\pi[1+(3e+3e^2+e^3)\sin^3\Phi]}$$

Figure 3. --Polar plot of strain.

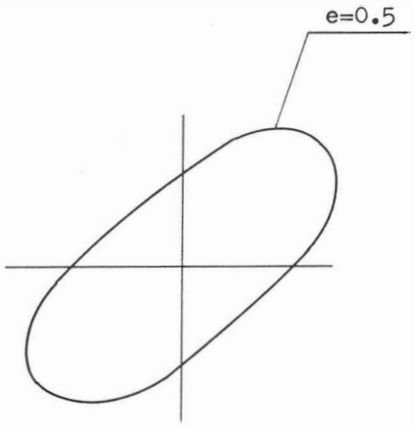

$e_{12}=e,\ e_{ij}=0 \text{ for } ij\neq 12$

$$\rho(\Phi)\triangleq \frac{1}{1-2e\sin\Phi\cos\Phi+e^2\sin^2\Phi}$$

Figure 4. --Polar plot of strain.

Turning briefly now to the case of splinter-shaped inclusions: the orientation of such particles is given simply by the coordinates "θ, ϕ" of the lines they lie along, as depicted in figure 6. After deformation then, the particle would lie along the line given by "θ', ϕ'." Assuming that the particle has some thickness, its trace on the xy-plane would be a "streak" in the "ϕ'" direction. It is convenient to call "ϕ'" the orientation of the streak; thus, one has:

$$\Phi = \phi' \tag{21}$$

Toward obtaining the transformation equations needed, let "x, y, Z" be a point on the line "θ, ϕ," then:

$$\begin{aligned} x &= r \sin\theta\cos\phi \\ y &= r \sin\theta\sin\phi \\ Z &= r \cos\theta \end{aligned} \tag{22}$$

By the deformation the point shifts to "x', y', Z'" on "θ', ϕ'":

$$\begin{aligned} x' &= r' \sin\theta' \cos\phi' \\ y' &= r' \sin\theta' \sin\phi' \\ Z' &= r' \cos\theta' \end{aligned} \tag{23}$$

From equations "22, 23, 6" one can write:

$$\tan\phi' = \frac{e_{21}\sin\theta\cos\phi + (1+e_{22})\sin\theta\sin\phi + e_{23}\cos\theta}{(1+e_{11})\sin\theta\cos\phi + e_{12}\sin\theta\sin\phi + e_{13}\cos\theta} \tag{24}$$

And from equation "21":

$$\Phi = \tan^{-1}\left[\frac{e_{21}\sin\theta\cos\phi + (1+e_{22})\sin\theta\sin\phi + e_{23}\cos\theta}{(1+e_{11})\sin\theta\cos\phi + e_{12}\sin\theta\sin\phi + e_{13}\cos\theta}\right] \tag{25}$$

Comparing equations "25" and "14" it is apparent that the two would be the same if the "e_{ij}" are replaced by the "a_{ij}" and "Φ" by "$\Phi - \pi$." Consequently, the probability distribution function "$\rho(\Phi)$" will be quite similar to that for flake-shaped particles. Indeed, for the strains considered in the figures (figs. 3 and 4), "$\rho(\Phi)$" has exactly the same form for both splinters and flakes. For the strain considered in figure 5, the probability distribution function would have a circular plot, indicating no alignment in the xy-plane. The curve presented in figure 5 would apply to splinter-shaped particles under the strain: $e_{13} = e$, $e_{ij} = 0$, $i, j \neq 1, 3$.

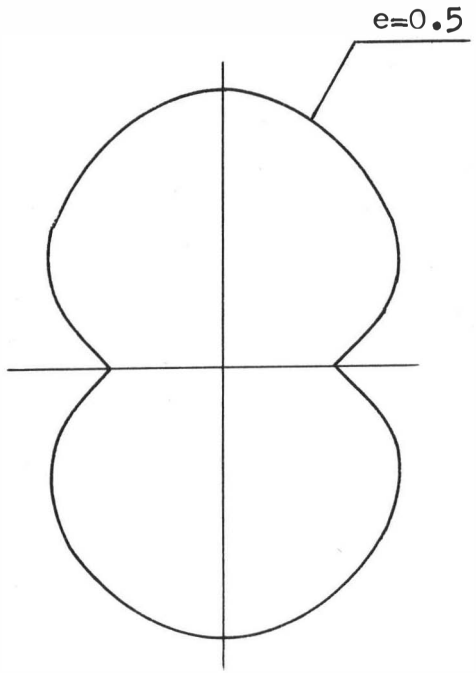

$$e_{31} = e, \quad e_{ij} = 0 \text{ for } ij \neq 31$$

$$\rho(\Phi) \doteq \frac{1}{1+e^2\cos^2\Phi}\left[1+\left(1+e^2\,\frac{1+e\cos\Phi}{\sin\Phi}\right)^{-\frac{1}{2}}\right]$$

Figure 5.--Polar plot of strain.

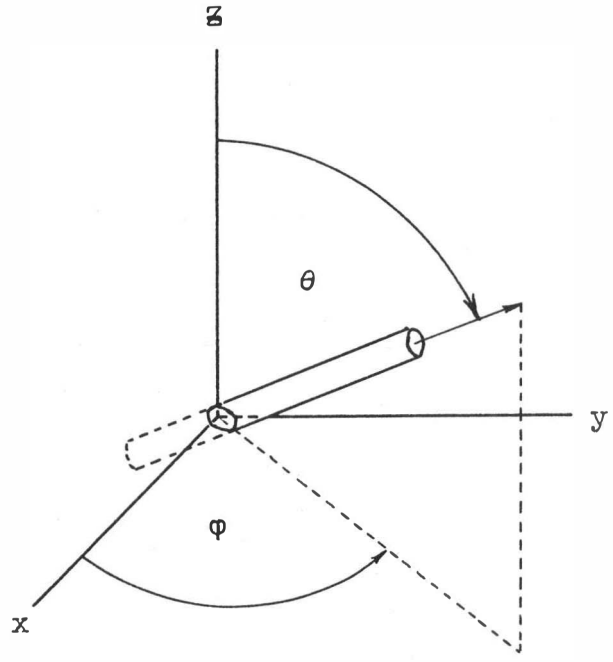

Figure 6.--Orientation of splinter-shaped particle.

The case of ellipsoidal inclusions was also considered, but less definite results were obtained due to the mathematical complexities involved. Besides the purely mathematical difficulty encountered in performing the integration required, the relationship between applied strain and change of orientation of the ellipsoid in the plastic medium is not at all obvious. One must assume some mechanism by which the "overall" strain of the medium effects the rotation of the inclusion. Two such mechanisms were considered by the author, both being valid only for small strains. The first treats the inclusions as being composed of a substance whose plastic properties are similar to those of the embedding medium. Calculation then follows the same scheme outlined for flake-shaped particles, with the formula for an ellipsoid replacing that for a plane. The planar orientation "Φ" would here be conveniently taken as the direction of the major axis of the ellipse cut out by the intersection of the ellipsoid, after deformation, with the xy-plane. The second method assumes that the embedding medium deforms as an elastic solid, the inclusion being rigid and in intimate contact with the medium. From the geological standpoint, this approximation would be particularly appropriate to the case where a very viscous magma is deformed in a relatively short period of time. In this second case, then, one must first solve the problem of a rigid ellipsoidal core welded into an infinite elastic medium, when the strain is given to be uniform at a great distance from the ellipsoid.

On the basis of some very specialized calculations carried out by the author along both lines discussed above, as well as from the results obtained previously for the cases of splinters and flakes, certain characteristics of the rose diagrams for ellipsoidal particles can be anticipated. It is expected that ellipsoidal inclusions with one axis much shorter than the other two would yield rose plots similar to that for flake-shaped particles but less eccentric for a given strain; the "thickness" tends to inhibit the rotation. And inclusions with one axis much greater than the other two would give a plot similar to that of splinters but again less eccentric. For ellipsoidal inclusions with less extreme dimensions, calculations have been carried only far enough to say that their rose plots will be quasielliptical and, of course, somewhat of a compromise between those of flake- and splinter-shaped inclusions.

APPLICATION

A comprehensive account of the structure of the Large Phenocryst Porphyry is given by Mayo (1961), including the results of a study on the distribution of crystal orientations. In what follows, two aspects of this distribution are examined: the significance of the individual rose diagram with regard to the number of crystals included in the measurements; and the variation between rose diagrams as taken at different places on the porphyry.

For ease in measuring crystal orientations, closeup photographs were taken of the various flat exposed surfaces of the porphyry to be studied. The surfaces chosen were either horizontal or vertical; the exposure of the vertical surfaces was either parallel or perpendicular to the axis of the formation. When a rose diagram was to be prepared, a centrally located crystal was selected on the photograph, and the orientation of its longest dimension was measured. The orientation of the longest dimension was then measured for every crystal in a circular region about the central one. Each measurement was then catalogued according to which of the 18 possible 10^{o} intervals it was oriented. The number of entries in each interval was plotted on polar paper

as a function of the midpoint angle of the interval. A smooth curve was then fitted to the points and closed by making use of the inversion symmetry property. Figure 7 shows schematically the arrangement of phenocrysts on a typical surface; a vertical longitudinal face was used to prepare this diagram, but similar features would be observed on any surface. No effort was made to preserve the exact size or shape of the individual phenocrysts, but the relative spacing is reproduced on a 1:1 scale. One of four symbols is assigned to each phenocryst according to which of the four apparent structural directions it tends to be oriented. The orientation of the largest dimension of each phenocryst in the figure corresponds, of course, to the orientation of the largest dimension of each actual phenocryst. The four structural directions are associated with the four maxima of the rose diagram for this surface, as drawn in the heavy smooth curve of figure 8. This curve is a smoothed out interpretation of the polygon shown in the same figure; the polygon was obtained by simply connecting the data points by straight lines. The distance of each data point from the center of the diagram is, of course, proportional to the number of phenocrysts in the 10^{o} interval in which the data point was plotted at the midpoint angle.

Two observations can be made regarding the distribution and orientation of phenocrysts in any given region: First, on measuring the orientations of all phenocrysts in successively larger and larger areas, the prominence of the maxima of the rose diagram is found to decrease but not to disappear. Second, as evidenced in figure 7, similarly oriented crystals are occasionally found concentrated in small irregular clusters. When this was first noticed the author was tempted to identify these groupings with shear planes truncated by other shear planes. But upon closer examination of the exposed areas on the porphyry, it appears impossible to discern any such structure; the clusters are distributed at random and cannot be associated with planes through the formation.

It has also been found that as one moves from place to place about the formation there is little change in the directional tendencies of the rose diagram maxima, although there can be considerable variation in the relative amplitudes. This variation depends partly on the exact area selected for measurement, because of statistical fluctuations, but mostly on the general region of the formation in which the measurements are being made. Figure 9 shows a map of the Large Phenocryst Porphyry; the rose diagrams are representative of the areas they overlie. It can be seen that there is a strong tendency for the phenocrysts to be aligned parallel to the contact of the formation. Also, the similarity between rose diagrams representative of the interior of the porphyry and those representative of the contacts seems to indicate that the mechanism responsible for the aligning was felt throughout the formation and not merely near the contacts. The information used in preparing this diagram was graciously supplied by Dr. Mayo and reproduces part of that presented in figure 3I of his paper (1961).

Figure 10 shows rose diagrams constructed on three mutually perpendicular surfaces; the rock surfaces represented were within a few feet of each other in the formation, their approximate location being indicated on the map in figure 9. In transposing from the little pulled-out block of figure 9 to the large cube of figure 10, the little block is imagined to be rotated so that the original east-northeast vertical face is toward the observer. The top surface of the large cube appears as though rotated clockwise through 90^{o}; otherwise it is identical with the top of the little block of figure 9. Due to a lack of suitably exposed vertical faces, little can be said about crystal alignment in

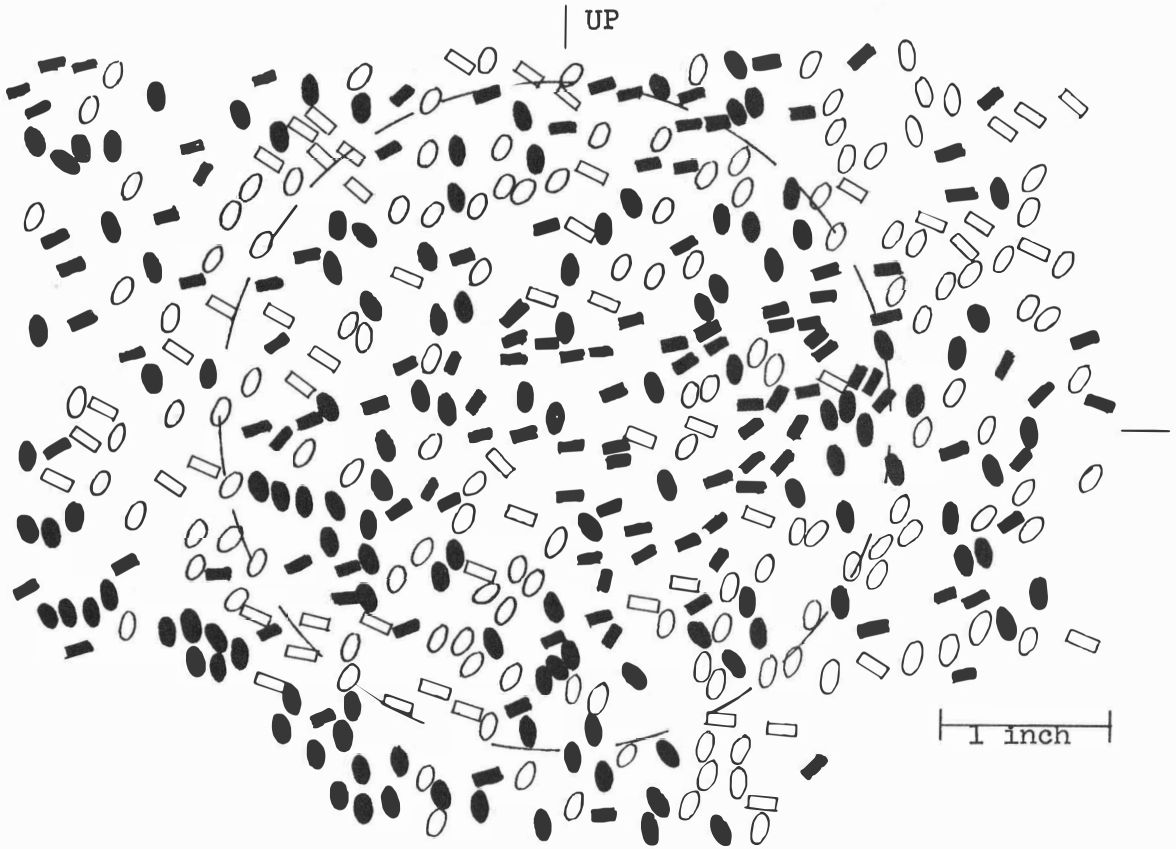

Figure 7. --Schematic diagram of arrangement of phenocrysts on a typical surface.

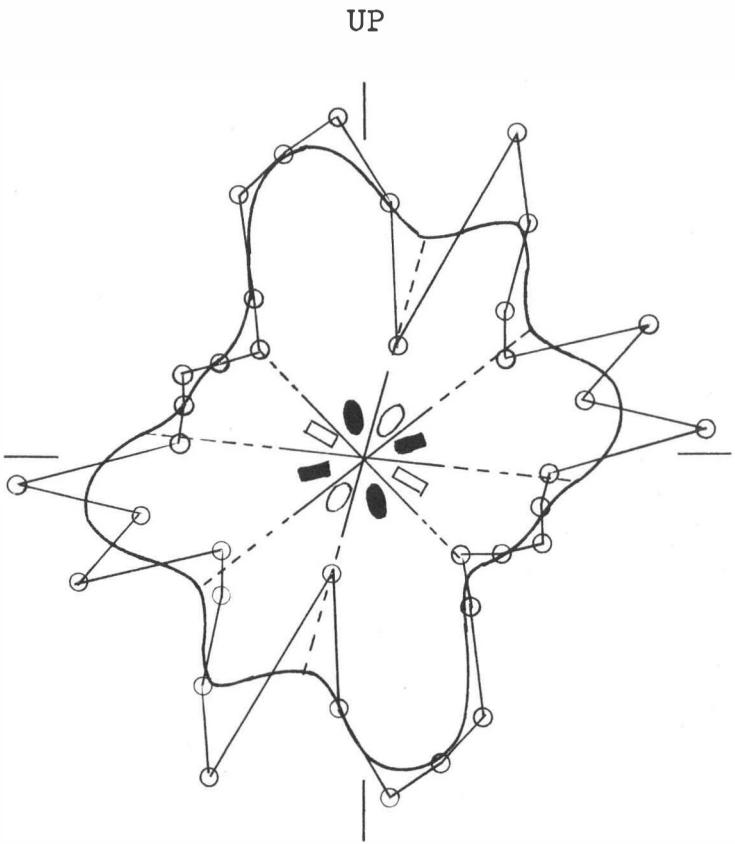

Figure 8. --Rose-diagram plot for data of figure 7.

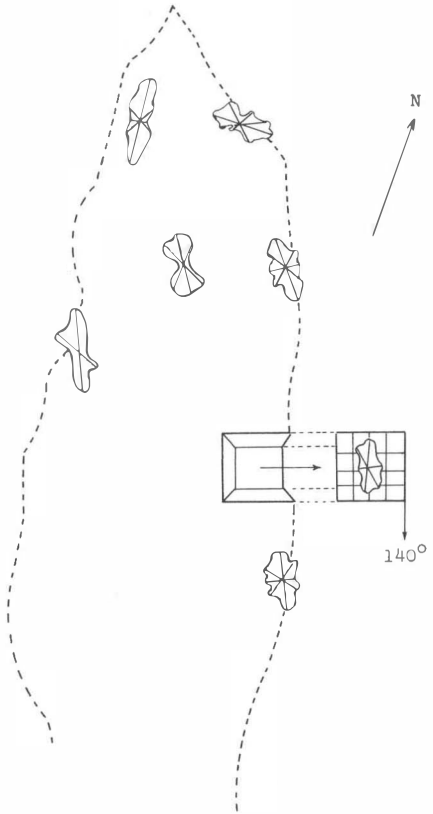

Figure 9. --Map of large phenocryst porphyry showing location of rose diagrams.

this dimension, but the information presented in figure 10 is representative of that obtained for the east-northeast contact.

Comparing the rose diagrams representative of the Large Phenocryst Porphyry with the theoretical curves derived earlier in this paper, it is obvious that the orientations of the crystals are not indicative of a pure affine deformation. Therefore, either an entirely different orienting mechanism must be sought as the sole explanation, or there must be a new mechanism acting together with affine deformation. Consider the latter alternative. If one looks only at the greatest maxima of the rose diagrams in figure 9, it could be inferred that the emplacement was effected by an upswelling of a very viscous magma in which the phenocrysts were suspended, accompanied by a squeezing out along the formation axis. This sort of deformation would be locally affine, and it is similar to the mechanism visualized by Mayo (1961). To explain the submaxima, then, two facts must be kept in mind. First, the directional tendencies of the maxima are similar over all the formation, suggesting that the structural mechanisms they reflect were effective during or after the emplacement. Second, similarly oriented crystals are occasionally found in small irregular clusters, casting doubt on the orienting influence of regular shear planes. Perhaps it can be imagined that after emplacement, but before final cooling, the formation was subjected to stresses that caused "incipient cracks" to develop in both the shear and tension positions—cracks which never evolved into extensive shear or joint planes. There would have been a tendency, then, for crystals to grow along such microcracks, and their intersections, producing the clustering observed. This suggested production of incipient cracks is reminiscent of the phenomena observed in brittle fracture where systems of tiny cracks permeate the stressed body in predictable directions before actual rupture occurs.

CONCLUSION AND ACKNOWLEDGMENTS

The interpretation arrived at above may crumble under future criticism, but as yet it does not seem to be inconsistent with known facts.

I would like to express my sincere thanks to Evans B. Mayo for his helpful comments and assistance rendered throughout the course of this work, to Arthur A. Evett for his advice on the mathematical formulation of the problem, and to my wife Loraine for her handling of the photographic details and help in preparation of the manuscript.

REFERENCES CITED

Riedel, Wolfgang, 1929, Das Aufquellen geologischer Schmelzmassen als plastischer Formanderungsvorgang: Neues Jahrb. Min., Geol., Pal., Beil. Bd. 62, Abt. B, p. 151-170.

March, Artur, 1932, Mathematische Theorie der Regelung nach der Korngestalt bei affiner Deformation: Zeitschrift fur Kristallographie, v. 81, p. 285-298.

Oertel, Gerhard, 1955, Theoretisches zu Bewegungen in Festen Korpern bei der Deformation: Geotektonische Forschungen, Heft 11, p. 84-107.

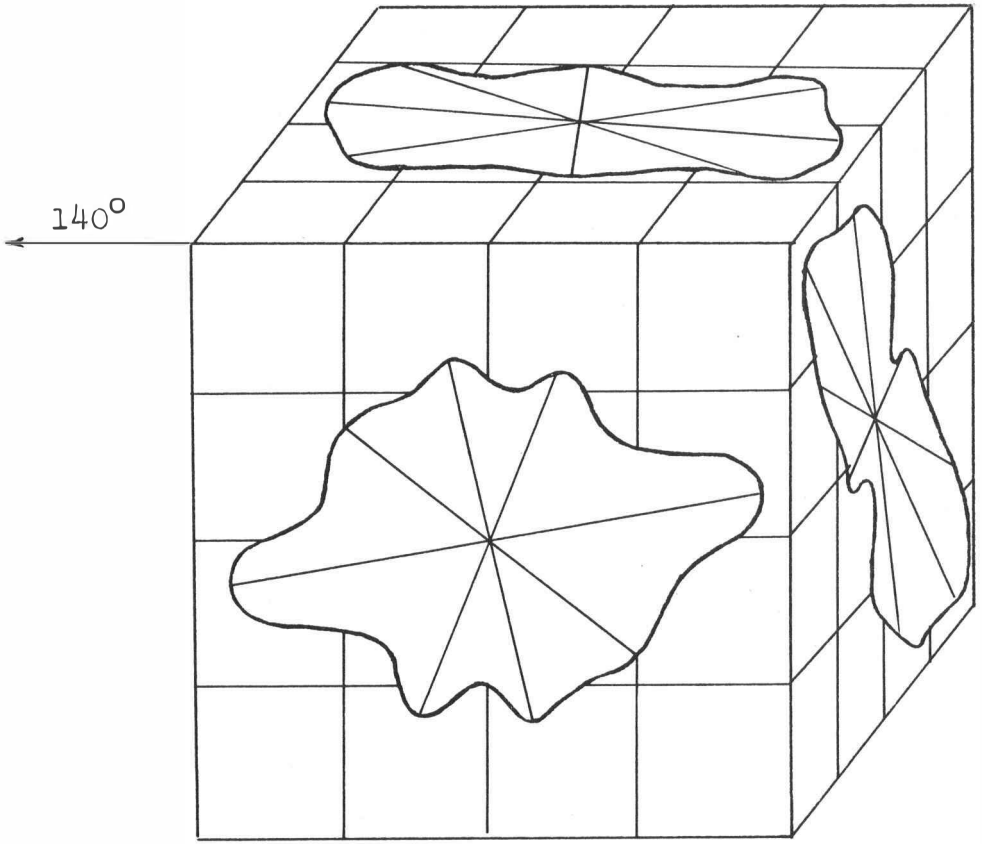

Figure 10.--Rose diagrams constructed on three mutually perpendicular surfaces.

Mayo, E. B., 1961, Structure of the Large Phenocryst Porphyry near Arizona-Sonora Desert Museum: Arizona Geol. Soc. Digest, v. 4, p. 1-15.

POSTSCRIPT

By

Evans B. Mayo

Department of Geology, University of Arizona

After reaching certain conclusions concerning the mode of emplacement of the Large Phenocryst Porphyry near the Arizona-Sonora Desert Museum, and on the possible mechanism by which its phenocrysts were oriented, it seemed advisable to have this problem studied by another investigator, using a different approach. Fortunately, Mr. Yeatts of the Department of Physics wished to apply his background of mathematics and physics to a geological problem. The result was the foregoing paper.

The problem is a very difficult one, and Mr. Yeatts deserves much credit for completing it. The tentative conclusion, that highly viscous molten masses pass through a stage of affine plastic deformation and enter a stage in which part of their phenocrysts become oriented to (grow along?) incipient shear or tension cracks, is important in studies of structures in granitic rocks. In such rocks crossed foliations are rather commonly found, suggesting crystal orientation along two or more well-developed sets of shear planes. Mr. Yeatt's results suggest that the phenomenon of crossed foliations could develop in congealing melts. In connection with other evidence, crossed foliations have also been used as a criterion of the metasomatic origin of certain granites.

The question of metasomatism vs. melts of extremely high viscosity should be of interest in connection with studies of related mineral deposits.